Editors' Suggestion

Third order corrections to the semileptonic $b \to c$ and the muon decays

Matteo Fael,[*] Kay Schönwald,[†] and Matthias Steinhauser[‡]
Institut für Theoretische Teilchenphysik, Karlsruhe Institute of Technology (KIT), 76128 Karlsruhe, Germany

(Received 4 December 2020; revised 2 February 2021; accepted 16 June 2021; published 6 July 2021)

We compute corrections of order α_s^3 to the decay $b \to c\ell\bar{\nu}$ taking into account massive charm quarks. In the on-shell scheme large three-loop corrections are found. However, in the kinetic scheme the three-loop corrections are below 1% and thus perturbation theory is well under control. We furthermore provide results for the order α_s^3 corrections to $b \to u\ell\bar{\nu}$ and the third-order QED corrections to the muon decay which will be important input for reducing the uncertainty of the Fermi coupling constant G_F.

DOI: 10.1103/PhysRevD.104.016003

I. INTRODUCTION

The Cabibbo-Kobayashi-Maskawa (CKM) matrix determines the mixing strength in the quark sector and provides furthermore the source for charge-parity (CP) violation in the Standard Model (SM). It is thus of prime importance to determine the parameters of the CKM matrix with highest accuracy. In this article we address the elements V_{ub} and V_{cb} which are accessible via semileptonic B meson decays.

At present, the value of $|V_{cb}|$ from inclusive $B \to X_c\ell\bar{\nu}$ decays is obtained from global fits [1–3]. The experimental inputs are the semileptonic width and the moments of kinematical distributions measured at Belle [4,5] and *BABAR* [6,7], together with earlier data from CDF [8], CLEO [9], and DELPHI [10]. The most recent determination in the so-called kinetic scheme $|V_{cb}| = (42.19 \pm 0.78) \times 10^{-3}$ [11] has a relative error of about 1.8%, which is mostly dominated by theoretical uncertainties. Global fits in the 1S scheme yield $|V_{cb}^{1S}| = (41.98 \pm 0.45) \times 10^{-3}$ [11,12].

A crucial ingredient for the determination of $|V_{ub}|$ and $|V_{cb}|$ is the total semileptonic decay rate. Branching ratios of inclusive semileptonic B mesons were measured at B factories with a relative precision of about 2.5% [4,13–15]. A relative uncertainty of 1.5% is obtained with the help of a global fit: $\mathrm{Br}(B \to X_c\ell^+\nu_\ell) = (10.65 \pm 0.16)\%$ [11]. Measurements are performed with a mild lower cut on the electron energy [4], which excludes less than 5% of the events, or extrapolated to the whole phase space based on Monte Carlo [13,14]. A key goal for Belle II is the reduction of the systematic uncertainties on the branching fraction determinations, as well as to obtain more precise and detailed measurements of $B \to X_c\ell\bar{\nu}_\ell$ differential distributions [16]. Recent analyses by Belle and Belle II of leptonic and hadronic invariant mass moments [17,18] show that a percent or even subpercent relative accuracy can be achieved for certain observables.

With the help of the heavy quark expansion the total rate can be written as a double series in α_s and $\Lambda_{\mathrm{QCD}}/m_b$. The m_b-suppressed corrections are obtained from higher-dimensional operators. In the free-quark approximation, corrections up to $\mathcal{O}(\alpha_s^2)$ are available [19–27] together with the leading β_0 terms at higher orders [28], where β_0 is the one-loop coefficient of the QCD beta function. The power corrections of order $\Lambda_{\mathrm{QCD}}^2/m_b^2$ and $\Lambda_{\mathrm{QCD}}^3/m_b^3$ have been computed in [29–32] to tree-level and in [33–36] to $\mathcal{O}(\alpha_s)$. Also $1/m_b^4$ and $1/m_b^5$ terms are known, however, only at leading order [37–40]. Note that linear $1/m_b$ corrections vanish to all orders. Missing higher-order perturbative and power corrections limit the current extraction of $|V_{cb}|$.

The relative size of the second order corrections to the partonic $b \to c\ell\bar{\nu}_\ell$ decays is about 1%–3% depending on the quark mass scheme, with a theoretical uncertainty due to renormalization scale variation estimated to be 1% [26], which soon can become comparable to experimental errors. In this work we make a major improvement in the theory underlying $B \to X_c\ell\bar{\nu}$ decays by computing the α_s^3 corrections to the total rate, at leading order in $1/m_b$. We incorporate a finite charm quark mass via an expansion in the mass difference $m_b - m_c$ and show that precise results can be obtained for the physical values of m_c and m_b. Our analysis even allows for the limit $m_c \to 0$

[*]matteo.fael@kit.edu
[†]kay.schoenwald@kit.edu
[‡]matthias.steinhauser@kit.edu

which provides α_s^3 corrections for the decay rate $\Gamma(B \to X_u \ell \bar{\nu})$.[1]

A process closely related to $b \to u\ell\bar{\nu}$ is the muon decay. Its lifetime, τ_μ, can be written in the following form

$$\frac{1}{\tau_\mu} \equiv \Gamma(\mu^- \to e^- \nu_\mu \bar{\nu}_e) = \frac{G_F^2 m_\mu^5}{192\pi^3}(1 + \Delta q), \qquad (1)$$

where G_F is the Fermi constant, m_μ is the muon mass and Δq contains QED and hadronic vacuum polarization corrections (see Ref. [41–43] for details). Note that all weak corrections are absorbed in G_F. Equation (1) allows for the determination of G_F if precise measurements of τ_μ are combined with accurate QED predictions. We compute for the first time α^3 corrections to Δq by specifying the color factors of our $b \to c\ell\bar{\nu}$ result to QED and taking the limit $m_c \to 0$. This allows for the determination of the third-order coefficient with an accuracy of 15%.

II. CALCULATION

We apply the optical theorem and consider the forward scattering amplitude of a bottom quark where at leading order the two-loop diagram in Fig. 1(a) has to be considered. It has a neutrino, a lepton and a charm quark as internal particles. The weak interaction is shown as an effective vertex. Our aim is to consider QCD corrections up to third order which adds up to three more loops. Some sample Feynman diagrams are shown in Fig. 1(b–f).

The structure of the Feynman diagrams allows the integration of the massless neutrino-lepton loop which essentially leads to an effective propagator raised to an ϵ-dependent power, where $d = 4 - 2\epsilon$ is the space-time dimension. The remaining diagram is at most of four-loop order.

From the technical point of view there are two basic ingredients which are crucial to realize our calculation. First, we perform an expansion in the difference between the bottom and charm quark mass. It has been shown in Ref. [27] that the expansion converges quite fast for the physical values of m_c and m_b. Second, we apply the so-called method of regions [44,45] and exploit the similarities to the calculation of the three-loop corrections to the kinetic mass [46].

The method of regions [44,45] leads to two possible scalings for each loop momentum k^μ

(i) $|k^\mu| \sim m_b$ (h, hard)
(ii) $|k^\mu| \sim \delta \cdot m_b$ (u, ultra-soft)

with $\delta = 1 - m_c/m_b$. We choose the notion "ultrasoft" for the second scaling to stress the analogy to the calculation of the relation between the pole and the kinetic mass of a heavy quark, see [46,47]. Note that the momentum which flows through the neutrino-lepton loop, ℓ, has to be ultrasoft since the Feynman diagram has no imaginary part if ℓ is hard since the corresponding on-shell integral has no cut.

Let us next consider the remaining (up to three) momentum integrations which can be interpreted as a four-point amplitude with forward-scattering kinematics and two external momenta: ℓ and the on-shell momentum $p^2 = m_b^2$. This is in close analogy to the scattering amplitude of a heavy quark and an external current considered in Ref. [46]. In fact, at each loop order each momentum can either scale as hard or ultrasoft:

$\mathcal{O}(\alpha_s)$	h, u
$\mathcal{O}(\alpha_s^2)$	hh, hu, uu
$\mathcal{O}(\alpha_s^3)$	hhh, hhu, huu, uuu

Note that all regions where at least one of the loop momenta scales ultrasoft leads to the same integral families as in Ref. [46,47]. The pure-hard regions were absent in [46,47]; they lead to (massive) on-shell integrals.

At this point there is the crucial observation that the integrands in the hard regions do not depend on the loop momentum ℓ. On the other hand, the ultrasoft integrals still depend on ℓ. However, for each individual integral the dependence of the final result on ℓ is of the form

$$(-2p \cdot \ell + 2\delta)^\alpha \qquad (2)$$

with known exponent α. This means that it is always possible to perform in a first step the ℓ integration which is of the form

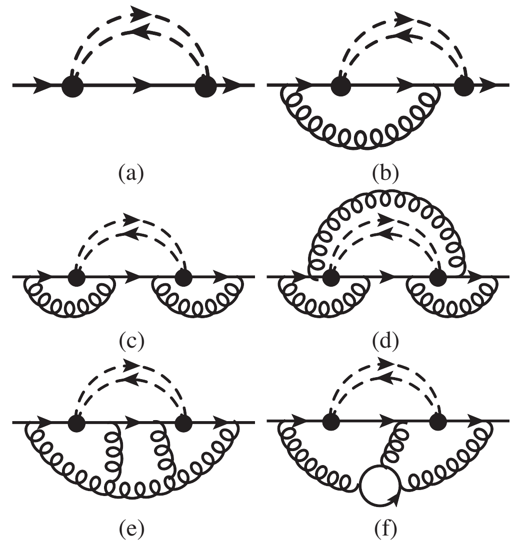

FIG. 1. Sample Feynman diagrams which contribute to the forward scattering amplitude of a bottom quark at LO (a), NLO (b), NNLO (c) and N^{3}LO (d-f). Straight, curly and dashed lines represent quarks, gluons and leptons, respectively. The weak interaction mediated by the W boson is shown as a blob.

[1]Note that in our approach one class of diagrams for the $b \to u$ transition is missing, namely the one where the charm quark appears as virtual particle in a closed loop. At $\mathcal{O}(\alpha_s^2)$ these corrections were denoted by U_C [22,23].

$$\int \mathrm{d}^d\ell \frac{\ell^{\mu_1}\ell^{\mu_2}\cdots}{(-2p\cdot\ell+2\delta)^\alpha(-\ell^2)^\beta}. \tag{3}$$

A closed formula for such tensor integrals with arbitrary tensor rank and arbitrary exponents α and β can easily be obtained from the formula provided in Appendix A of Ref. [45]. We thus remain with the loop integrations given in the above table. Similar to Eq. (3) we can integrate all one-loop hard or ultrasoft loops which leaves us with pure hard or pure ultrasoft contributions up to three loops.

A particular challenge of our calculation is the high expansion depth in δ. We perform an expansion of all diagrams up to δ^{12}. This leads to huge intermediate expressions of the order of 100 GB. Furthermore, for some of the scalar integrals individual propagators are raised to positive and negative powers up to 12, which is a nontrivial task for the reduction to master integrals. For the latter we combine FIRE [48] and LiteRed [49].[2] For the subset of integrals which are needed for the expansion up to δ^{10} we also use the stand-alone version of LiteRed [49] as a cross-check. For all regions where at least one of the regions is ultrasoft we can take over the master integrals from [46,47]. For some of the (complicated) three-loop triple-ultra-soft master integrals higher order ϵ terms are needed. The method used for their calculation and the results are given Ref. [47]. All triple-hard master integrals can be found in Ref. [50].

III. RESULTS

We write the total decay rate for the $b\to c$ transition in the form

$$\Gamma(B\to X_c\ell\bar{\nu})=\Gamma_0\left[X_0+C_F\sum_{n\geq 1}\left(\frac{\alpha_s}{\pi}\right)^n X_n\right]+\mathcal{O}\left(\frac{\Lambda^2_{\mathrm{QCD}}}{m_b^2}\right), \tag{4}$$

with $C_F=4/3$, $\Gamma_0=A_{\mathrm{ew}}G_F^2|V_{cb}|^2m_b^5/(192\pi^3)$, $X_0=1\text{–}8\rho^2-12\rho^4\log(\rho^2)+8\rho^6-\rho^8$ where $\rho=m_c^{\mathrm{OS}}/m_b^{\mathrm{OS}}$ and $\alpha_s\equiv\alpha_s^{(5)}(\mu_s)$ with μ_s being the renormalization scale. $A_{\mathrm{ew}}=1.014$ is the leading electroweak correction [51] and m_b^{OS} (m_c^{OS}) is the bottom (charm) pole mass. The one- and two-loop results are available from Refs. [20–27]. The main result of our calculation is X_3. In the following we set all color factors to their numerical values. Furthermore, we specify the number of massless quarks to 3 and take into account closed charm and bottom loops. For $\mu=m_b$ we have

$$X_3=\sum_{n\geq 5}x_{3,n}\delta^n, \tag{5}$$

with analytic coefficients $x_{3,n}$, which in general depend on $\log(\delta)$. For illustration purposes we show explicit results only for the leading term which for dimensional reasons is of order δ^5. Our result reads

$$C_Fx_{3,5}=\frac{533858}{1215}-\frac{20992a_4}{81}+\frac{8744\pi^2\zeta_3}{135}-\frac{6176\zeta_5}{27}-\frac{16376\zeta_3}{135}-\frac{2624l_2^4}{243}+\frac{5344\pi^2l_2^2}{1215}+\frac{179552\pi^2l_2}{405}-\frac{39776\pi^4}{6075}-\frac{1216402\pi^2}{3645}, \tag{6}$$

where $l_2=\log(2)$, $a_4=\mathrm{Li}_4(1/2)$ and ζ_n is the Riemann zeta function. Analytic results up to δ^{12} can be found in [52]. We note that the leading term given in Eq. (6) can be cross-checked against the results from [53] where the $b\to c$ transition has been computed in the limit $m_c=m_b$.[3]

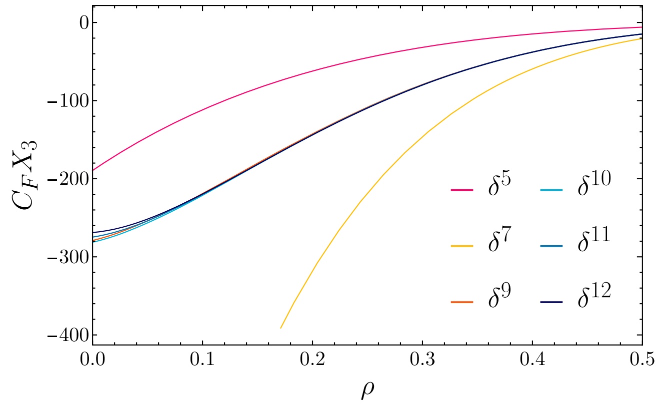

FIG. 2. The third-order coefficient (see Eq. (4)) as a function of $\rho=m_c^{\mathrm{OS}}/m_b^{\mathrm{OS}}$ for different expansion depth in δ.

In Fig. 2 we show X_3 as a function of $\rho=1-\delta=m_c^{\mathrm{OS}}/m_b^{\mathrm{OS}}$ where the different curves contain different expansion depths in δ. One observes a rapid convergence at the physical point for the $b\to c$ decay which amounts to $\rho\approx 0.3$. In particular, the curves including terms up to δ^{10}, δ^{11} or δ^{12} are basically indistinguishable for $\rho\approx 0.3$ which leads to $X_3(\rho=0.28)=-68.4\pm 0.3$, where the uncertainty is obtained from the difference of the δ^{11} and δ^{12} expansion, multiplied by a security factor of five.

For the numerical evaluation it is convenient to cast Eq. (4) in the form

$$\Gamma(B\to X_c\ell\bar{\nu})=\Gamma_0X_0\left[1+\sum_{n\geq 1}\left(\frac{\alpha_s}{\pi}\right)^n Y_n\right]+\mathcal{O}\left(\frac{\Lambda^2_{\mathrm{QCD}}}{m_b^2}\right), \tag{7}$$

with $\alpha_s\equiv\alpha_s^{(4)}(\mu_s)$ as expansion parameter. In the following we discuss various renormalization schemes for the charm and bottom quark masses, where Γ_0 and X_0 are evaluated

[2] We thank A. Smirnov for providing us with the private version of FIRE which was crucial for our calculation.

[3] After the submission of this paper, the authors of Ref. [54] independently confirmed the terms proportional to the C_F^3 and $C_Fn_h^2$ color factors up to δ^9.

TABLE I. Numerical results for the coefficients Y_n in Eq. (7) for various renormalization schemes.

	Y_1	$Y_2^{\rm rem}$	$\beta_0 Y_2^{\beta_0}$	$Y_3^{\rm rem}$	$\beta_0^2 Y_3^{\beta_0^2}$
$m_b^{\rm OS}, m_c^{\rm OS}$	−1.72	3.08	−16.17	48.8	−212.1
$m_b^{\rm kin}, m_c^{\rm kin}$	−0.94	0.33	−4.08	−5.4	−15.4
$m_b^{\rm kin}, \bar{m}_c(3\ \text{GeV})$	−1.67	−3.39	−3.85	−97.7	69.1
$m_b^{\rm kin}, \bar{m}_c(2\ \text{GeV})$	−1.25	−1.21	−2.43	−68.8	67.9
$\bar{m}_b(\bar{m}_b), \bar{m}_c(3\ \text{GeV})$	3.07	−21.81	35.17	−56.7	119.4
$m_b^{\rm PS}, \bar{m}_c(2\ \text{GeV})$	−0.47	−6.10	−2.31	−93.1	−7.19
$m_b^{\rm 1S}, \bar{m}_c(m_b^{\rm 1S})$	−3.59	−0.98	−19.39	−39.83	−80.22
$m_b^{\rm 1S}, m_c$ via HQET	−1.38	0.73	−7.05	5.04	−38.09

using the respective numerical values. In Table I we provide the corresponding results for the coefficients Y_n. At two and three-loop orders we split the results into the large-β_0 contribution and the remaining term

$$Y_2 = Y_2^{\rm rem} + \beta_0 Y_2^{\beta_0},$$
$$Y_3 = Y_3^{\rm rem} + \beta_0^2 Y_3^{\beta_0^2}, \tag{8}$$

with $\beta_0 = 11 - 2/3 n_l = 9$ where $n_l = 3$ is the number of massless quarks. Note that the uncertainty of Y_3 due to the expansion in δ is of the same order of magnitude as for X_3 discussed above.

For the transition of the on-shell quark masses to the $\overline{\rm MS}$ scheme we use the three-loop formulas provided in Refs. [55,56]. Finite-m_c effects in the bottom mass relation are taken from Refs. [57]. The two- and three-loop corrections to the transition from the on-shell to the kinetic scheme are provided in [58] and [46,47], respectively. Note that the transition to the kinetic scheme also requires the renormalization of the parameters μ_π^2 and ρ_D^3, which enter the decay rate at order $1/m_b^2$ and $1/m_b^3$, respectively. They receive additive contributions, which enter Y_i in Eq. (7) [59,60]. The corresponding corrections up to three-loop order can be found in [47]. Note that we assume a heavy charm quark and thus we have ($n_l = 3$)-flavor QCD as starting point for the on-shell–kinetic relations. We use the decoupling relation for α_s up to two-loop order to obtain expressions parametrized in terms of $\alpha_s^{(4)}$. For the decoupling scale we use μ_s. It has been shown in Ref. [47] that there are no additional charm quark mass effects in the kinetic-on-shell relation. For comparison we show in Tab. I also results where the bottom quark mass is renormalized in the PS [61] and 1S [62–64] scheme. In the latter case we renormalize the charm quark mass both in the $\overline{\rm MS}$ and via the heavy quark effective theory (HQET) relation to on-shell bottom quark mass and (averaged) D and B meson masses (see, e.g., Ref. [63]). After each scheme change we reexpand in α_s to third order.

Note that our two-loop results for $Y_2^{\rm rem}$ differ from the one of Ref. [2] due to finite charm quark mass effects in the relation between the kinetic and on-shell bottom quark mass and the renormalization of μ_π^2 and ρ_D^3 [47]. This leads to a shift of about −0.5% in the leading $1/m_b$ approximation of the decay rate and thus might have a visible effect on the value of $|V_{cb}|$.

For the numerical evaluation of the decay rate we use the input values $m_b^{\rm OS} = 4.7$ GeV, $m_c^{\rm OS} = 1.3$ GeV, $m_b^{\rm kin} = 4.526$ GeV, $m_b^{\rm PS} = 4.479$ GeV, $m_b^{\rm 1S} = 4.666$ GeV, $m_c^{\rm kin} = 1.130$ GeV, $\bar{m}_b(\bar{m}_b) = 4.163$ GeV, $\bar{m}_c(3\ \text{GeV}) = 0.993$ GeV, $\bar{m}_c(2\ \text{GeV}) = 1.099$ GeV, and $\alpha_s^{(5)}(M_Z) = 0.1179$. We use RunDec [65] for the running of the $\overline{\rm MS}$ parameters and the decoupling of heavy particles. For the Wilsonian cutoff in the kinetic scheme we use $\mu = 1$ GeV both for the bottom and charm quark. In the case of PS scheme we use $\mu = 2$ GeV. For the renormalization scale of $\alpha_s^{(4)}$, μ_s, we choose the respective value for the bottom quark mass.

For illustration purpose we provide in Table I also results where both masses are defined in the on-shell scheme. It is well known that in this scheme the perturbative series shows a bad convergence behavior. In fact, we have $Y_3 \approx -163$ whereas in the schemes where the bottom quark mass is used in the kinetic scheme we have that Y_3 is between −1 and −29. Note, that in the scheme where both quark masses are defined in the $\overline{\rm MS}$ scheme the three-loop corrections are more than twice as big which also hints for a worse convergence behavior. The PS and 1S schemes show a clear improvement as compared to the on-shell scheme. However, the convergence properties are significant worse than in the kinectic scheme in case the charm quark mass is renormalized in the $\overline{\rm MS}$ scheme. In case $m_c^{\rm OS}$ is expressed through $m_b^{\rm OS}$ and meson masses using a HQET relation one observes an improved perturbative behavior. Still, the analysis clearly shows the advantage of the kinetic scheme which is constructed such that large corrections are resummed into the quark mass value. In fact, all three schemes which involve $m_b^{\rm kin}$ demonstrate a good convergence behavior. Using $\alpha_s^{(4)}(m_b^{\rm kin}) = 0.2186$ we obtain for $\Gamma(B \to X_c \ell \bar{\nu})/\Gamma_0$ in these three schemes

$$\begin{aligned} m_b^{\rm kin}, m_c^{\rm kin} &: 0.633(1 - 0.066 - 0.018 - 0.007) \\ &\approx 0.575, \\ m_b^{\rm kin}, \bar{m}_c(3\ \text{GeV}) &: 0.700(1 - 0.116 - 0.035 - 0.010) \\ &\approx 0.587, \\ m_b^{\rm kin}, \bar{m}_c(2\ \text{GeV}) &: 0.648(1 - 0.087 - 0.018 - 0.0003) \\ &\approx 0.580, \end{aligned} \tag{9}$$

where the different α_s orders are displayed separately. Note that in the PS and 1S schemes the third-order corrections amount to 3.4% and 3.9%, respectively, with m_c in the $\overline{\rm MS}$ scheme. If one defines m_c in the 1S scheme via a HQET relation the third-order corrections reduce to 1%. For the bottom mass expressed in the kinetic scheme we observe that the third-order corrections amount to at most 1% and they are a factor two to three smaller than the corrections of order α_s^2. A particularly good behavior is observed for the choice $\bar{m}_c(2\ \text{GeV})$ where the corrections of order α_s^3 are below the per mille level. Its final result lies between the other two kinetic schemes and deviates from them by about 0.9% and 1.2%, respectively.

In Fig. 3 we show the partonic decay rate as a function of the renormalization scale μ_s. Figure 3(a) shows the bottom quark mass renormalized in the kinetic and the charm quark mass in the $\overline{\rm MS}$ scheme. One observes that over the whole range 2 GeV $< \mu_s <$ 10 GeV the dependence on μ_s decreases after including higher order corrections. (The LO order result is μ_s-independent by construction.) Whereas at NNLO one observes still a 2.5% variation, it is far below the percent level at N^{3}LO. Fig 3(b) shows the corresponding results for the 1S scheme where m_c is defined via a HQET relation.

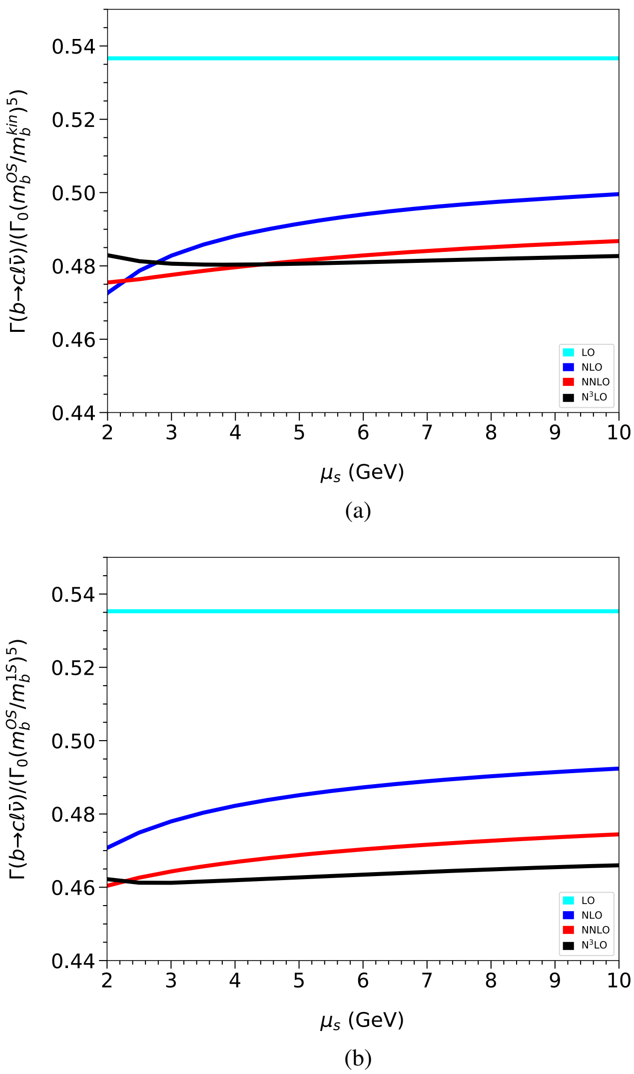

FIG. 3. Total partonic decay rate in the kinetic (a) and 1S scheme (b) as a function of the renormalization scale μ_s. See test for details. Note that the normalization chosen for the y axis is scheme independent.

The total partonic rate in the kinetic and in the 1S scheme differ for the following reason. Higher power corrections are not included in our partonic $b \to c\ell\bar{\nu}_\ell$ prediction. In particular the kinetic scheme absorbs μ^2/m_b^2 and μ^3/m_b^3 terms from the redefinition of μ_π^2 and ρ_D^3, while in the 1S scheme we neglect higher $1/m_b$ and $1/m_c$ power corrections when expressing the charm mass in terms of meson masses within HQET. Only the $B \to X_c\ell\bar{\nu}_\ell$ total rate predictions can be compared.

In general the large-β_0 terms provide dominant contributions. However, in all cases the remaining terms are not negligible and often have a different sign. In the kinetic scheme where the charm quark is renormalized in the $\overline{\rm MS}$ scheme the remaining contributions are numerically even bigger than the large-β_0 terms.

It is impressive that the expansion in δ shows a good converge behavior even for $\delta \to 1$ which corresponds to a massless daughter quark. This allows us to extract the coefficient X_3 for the decay $b \to u\ell\bar{\nu}$. A closer look to the δ^{10}, δ^{11}, and δ^{12} terms in Fig. 2 indicates that the convergence is quite slow for $\rho \to 0$. As central value for the three-loop prediction we use our approximation based on the δ^{12} term and estimate the uncertainty from the behavior of the one- and two-loop [66,67] results for $\rho = 0$, where the exact results are known. Incorporating expansion terms up to order δ^{12} we observe a deviation of about 3.5% whereas the δ^{12} terms amount to less than 1%, both at one and two loops. At three loops the δ^{12} term amounts to about 2%. We thus conservatively estimate the uncertainty to 10% which leads to

$$X_3^u \approx -202 \pm 20. \tag{10}$$

In this result the contributions with closed charm loops are approximated with $m_c = 0$.

In the remaining part of this paper we specify our results to QED and study the corrections to the muon decay. A comprehensive review of the various correction terms is given in Ref. [42] where Δq in Eq. (1) is parametrized as

$$\Delta q = \sum_{i\geq 0} \Delta q^{(i)}. \tag{11}$$

$\Delta q^{(0)}$ is given by $X_0 - 1$ [see Eq. (4)] with $\rho = m_e/m_\mu$ and $\Delta q^{(1)}$ [41] and $\Delta q^{(2)}$ [67,68] are easily obtained after specification of the QCD color factors to their QED values (see Ref. [42] for analytic results). We introduce $\Delta q^{(3)} = (\alpha(m_\mu)/\pi)^3 X_3^\mu$, where $\alpha(m_\mu)$ is the fine structure

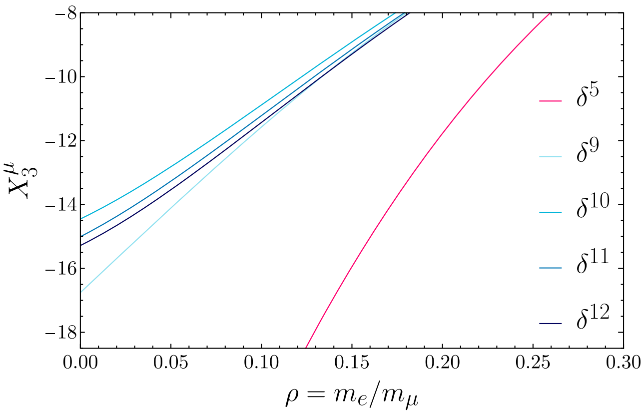

FIG. 4. The third-order coefficient to Δq introduced in Eq. (1) as a function of m_e/m_μ.

constant in the $\overline{\mathrm{MS}}$ scheme [42]. In Fig. 4 we show the third-order coefficient X_3^μ for $0 \leq \rho \leq 0.3$. At the physical point $m_e/m_\mu \approx 0.005$ the convergence behavior is similar to QCD. We estimate X_3^μ using the same approach as for X_3^u and examine the one- and two-loop behavior. Up to an overall factor C_F the one-loop term is, of course, identical to the $b \to u$ transition. Including expansion terms up to δ^{12} at two loops leads to a deviation by about 8% from the exact result whereas the δ^{12} term itself contributes by about 1%. The three-loop δ^{12} amounts to about 2%. Assuming the same relative contribution thus leads to an uncertainty estimate of about 15% and we have

$$\Delta q^{(3)} \approx \left(\frac{\alpha(m_\mu)}{\pi}\right)^3 (-15.3 \pm 2.3). \tag{12}$$

In Ref. [43] the three-loop corrections were estimated to $X_3^\mu \sim -20$. With the help of Eq. (1) we obtain for the α^3 QED contribution to the muon life time $(-9 \pm 1) \times 10^{-8}$ μs. This result has to be compared to the current experimental value which is given by $\tau_\mu = 2.1969811 \pm 0.0000022$ μs [69]. The new correction terms are almost two orders of magnitude smaller than the experimental uncertainty. Thus, an updated value of G_F can only be extracted once the latter has been improved.

IV. CONCLUSIONS

We have computed three-loop corrections of order α_s^3 to the total decay rate $\Gamma(B \to X_c \ell \bar{\nu})$ including finite charm quark mass effects. We perform an expansion around the equal-mass case and demonstrate that a good convergence at the physical point is observed after taking into account eight expansion terms. Our result is one of the very few third-order results to physical quantities available to date involving two different mass scales.

We can extend our considerations to the case of a massless charm quark and thus obtain corrections of order α_s^3 to $\Gamma(B \to X_u \ell \bar{\nu})$, although with a larger uncertainty of about 10%. After specifying our findings to QED we furthermore obtain predictions for the third-order corrections to the muon decay. Here we estimate the uncertainty to 15%.

The decay rate $\Gamma(B \to X_c \ell \bar{\nu})$ is an important ingredient for the determination of the CKM matrix element $|V_{cb}|$. However, a detailed analysis (see, e.g., Ref. [2]) also requires the knowledge of moments of kinematic distributions. The method described in this paper can also be applied to the calculation of such moments at order α_s^3, although at the cost of significantly increased computer resources.

ACKNOWLEDGMENTS

We thank Paolo Gambino for communications and clarifications concerning Ref. [2]. We are grateful to Alexander Smirnov for his support in the use of FIRE and to Florian Herren for providing us his program LIMIT [70] which automates the partial fraction decomposition in case of linearly dependent denominators. We thanks Joshua Davies for valuable advice in optimizing the usage of FORM [71]. This research was supported by the Deutsche Forschungsgemeinschaft (DFG, German Research Foundation) under Grant No. 396021762—TRR 257 "Particle Physics Phenomenology after the Higgs Discovery".

[1] P. Gambino and C. Schwanda, Phys. Rev. D **89**, 014022 (2014).
[2] A. Alberti, P. Gambino, K. J. Healey, and S. Nandi, Phys. Rev. Lett. **114**, 061802 (2015).
[3] P. Gambino, K. J. Healey, and S. Turczyk, Phys. Lett. B **763**, 60 (2016).
[4] P. Urquijo *et al.* (Belle Collaboration), Phys. Rev. D **75**, 032001 (2007).
[5] C. Schwanda *et al.* (Belle Collaboration), Phys. Rev. D **75**, 032005 (2007).
[6] B. Aubert *et al.* (*BABAR* Collaboration), Phys. Rev. D **69**, 111104 (2004).
[7] B. Aubert *et al.* (*BABAR* Collaboration), Phys. Rev. D **81**, 032003 (2010).
[8] D. Acosta *et al.* (CDF Collaboration), Phys. Rev. D **71**, 051103 (2005).

[9] S. E. Csorna *et al.* (CLEO Collaboration), Phys. Rev. D **70**, 032002 (2004).
[10] J. Abdallah *et al.* (DELPHI Collaboration), Eur. Phys. J. C **45**, 35 (2006).
[11] Y. S. Amhis *et al.* (HFLAV Collaboration), Eur. Phys. J. C **81**, 226 (2021).
[12] C. W. Bauer, Z. Ligeti, M. Luke, A. V. Manohar, and M. Trott, Phys. Rev. D **70**, 094017 (2004).
[13] J. P. Lees *et al.* (*BABAR* Collaboration), Phys. Rev. D **95**, 072001 (2017).
[14] A. H. Mahmood *et al.* (CLEO Collaboration), Phys. Rev. D **70**, 032003 (2004).
[15] H. Albrecht *et al.* (ARGUS Collaboration), Phys. Lett. B **318**, 397 (1993).
[16] E. Kou *et al.* (Belle-II Collaboration), Prog. Theor. Exp. Phys. (**2019**), 123C01; (**2020**), 029201(E).
[17] R. van Tonder (Belle Collaboration), arXiv:2105.08001.
[18] F. Abudinén *et al.* (Belle-II Collaboration), arXiv: 2009.04493.
[19] M. E. Luke, M. J. Savage, and M. B. Wise, Phys. Lett. B **345**, 301 (1995).
[20] M. Trott, Phys. Rev. D **70**, 073003 (2004).
[21] V. Aquila, P. Gambino, G. Ridolfi, and N. Uraltsev, Nucl. Phys. **B719**, 77 (2005).
[22] A. Pak and A. Czarnecki, Phys. Rev. Lett. **100**, 241807 (2008).
[23] A. Pak and A. Czarnecki, Phys. Rev. D **78**, 114015 (2008).
[24] K. Melnikov, Phys. Lett. B **666**, 336 (2008).
[25] S. Biswas and K. Melnikov, J. High Energy Phys. 02 (2010) 089.
[26] P. Gambino, J. High Energy Phys. 09 (2011) 055.
[27] M. Dowling, J. H. Piclum, and A. Czarnecki, Phys. Rev. D **78**, 074024 (2008).
[28] P. Ball, M. Beneke, and V. M. Braun, Phys. Rev. D **52**, 3929 (1995).
[29] J. Chay, H. Georgi, and B. Grinstein, Phys. Lett. B **247**, 399 (1990).
[30] I. I. Y. Bigi, M. A. Shifman, N. G. Uraltsev, and A. I. Vainshtein, Phys. Rev. Lett. **71**, 496 (1993).
[31] A. V. Manohar and M. B. Wise, Phys. Rev. D **49**, 1310 (1994).
[32] M. Gremm and A. Kapustin, Phys. Rev. D **55**, 6924 (1997).
[33] T. Becher, H. Boos, and E. Lunghi, J. High Energy Phys. 12 (2007) 062.
[34] A. Alberti, P. Gambino, and S. Nandi, J. High Energy Phys. 01 (2014) 147.
[35] T. Mannel, A. A. Pivovarov, and D. Rosenthal, Phys. Lett. B **741**, 290 (2015).
[36] T. Mannel and A. A. Pivovarov, Phys. Rev. D **100**, 093001 (2019).
[37] B. M. Dassinger, T. Mannel, and S. Turczyk, J. High Energy Phys. 03 (2007) 087.
[38] T. Mannel, S. Turczyk, and N. Uraltsev, J. High Energy Phys. 11 (2010) 109.
[39] T. Mannel and K. K. Vos, J. High Energy Phys. 06 (2018) 115.
[40] M. Fael, T. Mannel, and K. Keri Vos, J. High Energy Phys. 02 (2019) 177.
[41] T. Kinoshita and A. Sirlin, Phys. Rev. **113**, 1652 (1959).
[42] T. van Ritbergen and R. G. Stuart, Nucl. Phys. **B564**, 343 (2000).
[43] A. Ferroglia, G. Ossola, and A. Sirlin, Nucl. Phys. **B560**, 23 (1999).
[44] M. Beneke and V. A. Smirnov, Nucl. Phys. **B522**, 321 (1998).
[45] V. A. Smirnov, Springer Tracts Mod. Phys. **250**, 1 (2012).
[46] M. Fael, K. Schönwald, and M. Steinhauser, Phys. Rev. Lett. **125**, 052003 (2020).
[47] M. Fael, K. Schönwald, and M. Steinhauser, Phys. Rev. D **103**, 014005 (2021).
[48] A. V. Smirnov and F. S. Chuharev, Comput. Phys. Commun. **247**, 106877 (2020).
[49] R. N. Lee, arXiv:1212.2685; R. N. Lee, J. Phys. Conf. Ser. **523**, 012059 (2014).
[50] R. N. Lee and V. A. Smirnov, J. High Energy Phys. 02 (2011) 102.
[51] A. Sirlin, Nucl. Phys. **B196**, 83 (1982).
[52] https://www.ttp.kit.edu/preprints/2020/ttp20-042/.
[53] J. P. Archambault and A. Czarnecki, Phys. Rev. D **70**, 074016 (2004).
[54] M. L. Czakon, A. Czarnecki, and M. Dowling, Phys. Rev. D **103**, L111301 (2021).
[55] K. G. Chetyrkin and M. Steinhauser, Nucl. Phys. **B573**, 617 (2000).
[56] K. Melnikov and T. v. Ritbergen, Phys. Lett. B **482**, 99 (2000).
[57] M. Fael, K. Schönwald, and M. Steinhauser, J. High Energy Phys. 10 (2020) 087.
[58] A. Czarnecki, K. Melnikov, and N. Uraltsev, Phys. Rev. Lett. **80**, 3189 (1998).
[59] D. Benson, I. I. Bigi, T. Mannel, and N. Uraltsev, Nucl. Phys. **B665**, 367 (2003).
[60] P. Gambino, P. Giordano, G. Ossola, and N. Uraltsev, J. High Energy Phys. 10 (2007) 058.
[61] M. Beneke, Phys. Lett. B **434**, 115 (1998).
[62] A. H. Hoang, Z. Ligeti, and A. V. Manohar, Phys. Rev. D **59**, 074017 (1999).
[63] A. H. Hoang, Z. Ligeti, and A. V. Manohar, Phys. Rev. Lett. **82**, 277 (1999).
[64] A. Hoang and T. Teubner, Phys. Rev. D **60**, 114027 (1999).
[65] F. Herren and M. Steinhauser, Comput. Phys. Commun. **224**, 333 (2018).
[66] T. van Ritbergen, Phys. Lett. B **454**, 353 (1999).
[67] M. Steinhauser and T. Seidensticker, Phys. Lett. B **467**, 271 (1999).
[68] T. van Ritbergen and R. G. Stuart, Phys. Rev. Lett. **82**, 488 (1999).
[69] M. Tanabashi *et al.* (Particle Data Group), Phys. Rev. D **98**, 030001 (2018).
[70] F. Herren, Precision calculations for Higgs boson physics at the LHC—Four-loop corrections to gluon-fusion processes and higgs boson pair-production at NNLO, Ph.D. thesis, KIT, 2020.
[71] B. Ruijl, T. Ueda, and J. Vermaseren, arXiv:1707.06453.